applied sciences

MDPI

Article

An Experimental Study on the Injection Characteristics and the Macroscopic Spray Characteristics of Rapeseed Oil-Diesel Fuel Blends

Stasys Slavinskas

Department of Mechanical, Energy and Biotechnology Engineering, Faculty of Engineering, Agriculture Academy, Vytautas Magnus University, 53361 Kaunas, Lithuania; stasys.slavinskas@vdu.lt

Abstract: In this study, the injection processes and spray behavior of diesel fuel (DF), rapeseed oil (RO) and their fuel blends (RO25, RO50, RO75) have been qualitatively and quantitatively analyzed to identify the differences in the injection rate and the spray parameters. The volumetric and mass injection rates, the spray penetration, the spray cone angle and the spray area under non-evaporation conditions in a nitrogen-filled camber were analyzed. The results showed that rapeseed oil leads to a decrease in the peak injection rate due to its higher density and viscosity. Moreover, rapeseed oil and its blends with mineral diesel oil exhibited smoother rising slopes at the start of injection. The spray tip penetration was the longest for the rapeseed oil and the spray tip penetrations of the fuel blends RO25, RO50 and RO75 were arranged between the values of DF and RO. As the injection pressure increased, the differences in the spray tip penetrations diminished. Increasing the amount of rapeseed oil in fuel blends resulted in a smaller spray cone angle compared to diesel fuel. The spray area of all tested fuels increased significantly with increasing spray tip penetration, the spray area of RO was consistently lower than that of diesel fuel.

Keywords: diesel injection; injection rate; macroscopic spray characteristics; rapeseed

check for updates

Citation: Slavinskas, S. An Experimental Study on the Injection Characteristics and the Macroscopic Spray Characteristics of Rapeseed Oil-Diesel Fuel Blends. *Appl. Sci.* **2023**, *13*, 5944. https://doi.org/10.3390/app13105944

Academic Editors: Dariusz Szpica, Andrzej Borawski and Grzegorz Mieczkowski

Received: 5 April 2023
Revised: 2 May 2023
Accepted: 8 May 2023
Published: 11 May 2023

Copyright: © 2023 by the author. Licensee MDPI, Basel, Switzerland. This article is an open access article distributed under the terms and conditions of the Creative Commons Attribution (CC BY) license (https://creativecommons.org/licenses/by/4.0/).

1. Introduction

The world G20 leaders' summit in Rome and the UN COP26 conference in Glasgow endorsed zero carbon emissions by mid-century for limiting global warming to 1.5 °C is considered the last chance to rescue the planet. A big number of diesel engines, fuel-energy demand and global warming encourage scientists to search for renewable and locally available biofuels. The US Departments of Energy (USDOE) and Agriculture (USDA) define sustainable biofuels as those that are "economically competitive, conserve the natural resource base, and ensure social well-being" [1]. Diesel engines fueled with vegetable oils can reduce CO_2 emissions by nearly 60% in a global cycle to prevent climate change through the decarbonization of agricultural and transport sectors. Pure rapeseed (canola) oil as a diesel fuel substitute has the potential to reduce production and transportation expenditures even more significantly with the elimination of air/water pollution because the esterification facilities and biodiesel washing and drying at the temperature of about 105 °C are no longer needed to remove residual methanol and glycerol before transferring for end-use or distribution [1].

As stated at the 30th European Biomass Conference EUBCE 2022, sustainable biomass is the indisputable leading renewable energy source for the global consumer to play a critical role in the decarbonization process of the world economy. A green energy strategy focused on the use of vegetable oils in remote farms, peninsulas, and ecologically sensitive regions suggests a huge economic potential for local agricultural enterprises due to the decentralization of the fuel supply chain. Vegetable oil is especially of interest to farmers because it can be extracted from harvested crops almost for free during on-farm production of oilseed cakes for animal breeding. Using crude oil in a diesel engine reduces

production costs, energy losses for transportation and ambient air pollution. Additionally, it is important to stress that the energy used for biomass production, conversion, and utilization should be less than the energy content of the final product [1]. As a cheap, locally available, totally renewable, safe to handle and store, environmentally friendly owing to low sulfur and aromatic content fuel-energy source, pure rapeseed oil traditionally has been most popular among other vegetable oils and, therefore, can be regarded as a potential diesel fuel substitute.

Directive (EU) 2018/2001 of the European Parliament and of the Council of 11 December 2018 on the promotion of the use of energy from renewable sources tolerates greater flexibility for the Member States to meet their greenhouse gas reduction targets in the most cost-effective manner following their specific circumstances, energy mix and capacity to produce renewable energy. A diverse array of vegetable oils extracted from domestically grown crops, especially rapeseed and soybean, can be used for diesel engine fuelling. The use of locally produced pure rapeseed oil (RO) that complies with the fuel standard DIN 51605:2020-11 [2] is the cheapest way to reduce carbon dioxide (CO_2) emissions in a global cycle and contribute to protecting the climate.

Fridrihsone et al. [3] performed a life cycle assessment (LCA) of rapeseed produced in Latvia to update the LCA model based on an up-to-date agricultural practice in Northern Europe. They found that total greenhouse gas (GHG) emissions are 1268 kg CO_2 eq./t to produce spring rapeseed and 1064 kg CO_2 eq./t for winter rape. Whereas total GHG emissions from rapeseed cultivation to processing vary within the range of 203.7–354.7 kg CO_2 eq./t in Slovenia to 828.5–5904.2 kg CO_2 eq./t in Italy. It depends on the vegetable type, life cycle inventory methods and other factors. Nevertheless, rapeseed contains a high oil ratio of 37–50% [4], therefore, its use in diesel engines is economically feasible and can contribute to reducing CO_2 emissions in a global cycle.

However, the injection and spray macroscopic characteristics of pure RO and its blends with commercial diesel fuel are among the most important factors playing a critical role in diesel engine performance and emissions.

The primary purpose of atomization is to increase the surface area of the biofuel and thereby enhance its intensity of evaporation which is vital for achieving the desired rates of heat and mass transfer from the surrounding gases to the fuel. Lefebvre and McDonell [5] also emphasize that the properties of a liquid most relevant to atomization are surface tension, viscosity, and density. These fuel properties may have an impact on the flow rate, the velocity of the liquid jet and the parameters of fuel spray patterns as well. A fully turbulent jet breaks up into a multiplicity of small drops when the consolidating surface tension forces are overcome by aerodynamic or pressure forces. The spray attributes include cone angle, penetration, and radial and circumferential liquid distribution.

While Han et al. [6] studied the injection process of three fatty acid esters and diesel fuel on a CR system. They found that the injection rate increased with the injection pressure ranging from 45 to 100 MPa due to the enhanced flow capacity. Methyl laurate, and methyl and ethyl oleates produced lower volumetric injection quantities, but their higher density ensured a greater mass cycle injection quantity than diesel.

Vojtišek-Lom et al. [7] studied the behavior of diesel fuel and RO in a tractor diesel engine with an in-line fuel injection pump for various fuel heating temperatures, engine loads and speeds. They observed that the injection pressure rises earlier before TDC with decreasing fuel temperature due to faster propagation of pressure waves that partially compensate for long ignition delay at lower loads and advances the start of combustion at higher loads. Peak injection pressures were higher for heated (70–80 °C) RO than for diesel fuel at the same (10%) load and nearly comparable at full (100%) engine load. The earlier start of injection (SOI) and higher injection pressures have the potential to offset the poorer atomization and evaporation of RO at lower loads.

Ettl et al. [8] evaluated rapeseed oil (R100) as a renewable fuel for agricultural machinery based on long-term operation behavior and emissions of a fleet of tractors over more than 50,000 operation hours under Bavarian farm conditions. The tractors demonstrated

their full functionality, and no serious engine failures were observed, while minor malfunctions and repairs occurred just occasionally. The reliability of the tractors running on rapeseed oil was comparable to that of tractors running on diesel fuel, with no indication of engine deterioration. The 18 tractors running on R100 saved about 220 tonnes of CO_2 eq per year on average from 2015 to 2017. RO is biodegradable, non-toxic, safe to store and handle, and especially suitable for agricultural applications.

Low kinematic viscosity, high cetane number diethyl carbonate (DEC) as low price and renewable nature oxygenated additive (solvent) can be used to adjust the viscosity of diesel fuel and castor oil (CO) or sunflower oil (SVO) blends, improve the ignition quality, operating properties of a diesel engine on double DEC/SVO and triple D/DEC/SVO fuel blends, achieve low emissions and reduce smoke density by nearly 92–95% [9]. This method can improve the poor atomization of crude vegetable oil and reduce the formation of deposits in the cylinder. However, blending fuels of various origins and the increased aging process during storage of these blends can provide some difficulties in practical aspects.

Hanna and Zoughaib [10] investigated the atomization of liquids within the viscosity range of 55.9–134.9 mm^2/s (involving that of crude rapeseed oil) through swirl hydraulic atomizers to evaluate the changes in the mass flow rate, the discharge coefficient, and the atomization quality. They showed that the discharge coefficient of nozzle orifices and the mass flow rate depend on the Reynolds number. Additionally, spray droplets become smaller with increasing injection pressure and oil temperature, which effectively decreases oil viscosity as the major contributing factor to the improved break up of the spray.

Galle et al. [11] conducted single-shot injection experiments with a pump-line-nozzle injection system in an optically accessible constant volume combustion chamber filled with inert gas, N_2, at a maximum pressure of 80 bar and temperature of 150 °C. They studied the influences of physical fuel properties, engine speed and in-cylinder conditions on the injection pressure, needle lift, spray length, cone angle and atomization using diesel fuel, rapeseed biodiesel, rapeseed oil, palm oil and animal fats. The higher bulk modulus of straight vegetable oil and animal fat resulted in an earlier and faster needle lift, while higher density led to longer injection duration, slightly faster spray penetration and worse atomization compared to diesel and RME with similar spray angles for different fuels.

Das et al. [12] found that the higher viscosity and surface tension of castor oil, neem oil and sunflower oil increases the Sauter mean diameter values 2.4, 1.4 and 1.1 times and on the contrary, decreases the cone angle of the spray in comparison to petroleum diesel fuel at the injection pressure of 200 bar and air density of 25 kg/m^3.

Vice versa, the lower viscosity of oxygenated fuels plays a positive effect on the atomization quality; therefore, these fuels show larger spray cone angles and shorter spray tip penetration (STP). While biodiesel shows longer STP, larger peak velocity of the spray tip and smaller SCA compared to diesel [13]. This may happen because biodiesel's relatively higher density and viscosity are not conducive to improving the liquid spray and promoting the mixture.

Xie et al. [14] investigated the spray characteristics of different blends of biodiesel derived from drainage oil and diesel BD20, BD50, BD80, and BD100 under different injection (60–100 MPa) and ambient (0.1–0.9 MPa) pressures using CR system equipped with a constant volume chamber. They found that as increased injection pressure was increased, spray tip penetration, spray angle, spray area and spray volume increased. Increased ambient pressure led to the spray angle increasing, but the spray tip penetration and the peak of average tip velocity decreased. Viscosity and surface tension were the main physical properties affecting liquid jet breakup and atomization.

Tests of Residual Fuel Oil (RFO) showed that the spray area and its volume are not affected by changes in the fuel viscosity and surface tension, these parameters increase with the injection time mainly [15]. The higher viscosity of RFO than that of diesel increased penetration length, while the spray cone angle decreased at higher viscosity values for both fuels.

Further investigations by Wang et al. [16] showed that low fuel temperature causes longer injection delays, shorter injection duration, lower mass flow rate and less fuel mass injected. The low fuel temperature can effectively suppress the occurrence of cavitation, which accelerates the transition from cavitating to turbulent flow and then to laminar flow with a decrease in injection pressure. The discharge coefficient was affected more by the fuel viscosity at low temperature (−18 °C) than by the injector's structure, but the low temperature and injection pressure changed the laminar flow and, thus, the discharge coefficient decreased.

Payri et al. [17] conducted an experimental and computational investigation in a CR DI system to evaluate the influence of the physical properties of biodiesel (RME) on the injection process (mass flow rate) and the behavior of the system under multi-injection strategies. The use of RME affected the dynamic response of the needle, especially at low injection pressures, becoming less important at high injection pressure, compared to diesel fuel. The higher viscosity of biodiesel slowed down the opening and closing of the injector needle, the flow regime, and the discharge coefficient of the nozzle's orifices.

Salvador et al. [18] continued experiments with a one-dimensional model of a solenoid injector using the same fuels. They showed that the needle velocity during the opening is significantly lower for the biodiesel fuel; therefore, more time is needed to reach its maximum lift compared to diesel fuel. The needle lifts and the mass flow rates were also lowered for the RME, especially during the opening slope of the curve. This fact was attributed to the lower Reynold's number due to the higher viscosity of RME, which increases the friction force, affecting the needle dynamics. The dynamic delay was higher, and the start of combustion occurred about 160 μs later for biodiesel at 40 MPa but it decreased to 15 or 20 μs for higher injection pressures of 80–180 MPa under single-shot strategies.

Bohl et al. [19] studied the spray characteristics of hydrotreated vegetable oil (HVO), and three vegetable oil methyl esters (FAME) using a direct photography technique to compare with those of reference diesel fuel. They found that high-density fuels such as FAMEs have longer spray penetrations than mineral diesel, whereas HVO with the lowest density achieves the shortest penetration distance (by 5%) and slightly higher cone angle.

Ghurii et al. [20] studied the effects of diesel fuel D100 and biodiesel-diesel blends BD25, BD45 and BD65 on the spray tip penetration (STP) and cone angle of the sprays injected by a CR system at the injection pressures of 40–100 MPa into the atmospheric chamber. They depicted that the STP grows more than two times quicker before break-up than after break-up time. Even though the initial STP of D100 is always longer, the higher viscosity and momentum of biodiesel assure a slightly longer STP length than that of diesel with a little narrower spray angle (BD65) at 2.5 μs after the start of injection.

Boundy et al. [21] studied the impact of biodiesel properties on the injection characteristics of the common-rail system and discovered that fuel density is the main property that affects the mass amount of injected fuel and pressure wave in the CR system. They showed that pressure wave amplitude decreases with increasing fuel viscosity, bulk modulus, or density.

It is interesting to notice that Dernotte et al. [22], studying the influence of density and viscosity of nine fuel types (light and dense) on the pressure wave characteristics produced by a high-pressure CR diesel injector with three conical convergent orifices, declared similar findings. They showed that with the increase in viscosity from 0.6 to 7.0 mm^2/s the discharge coefficient decreases by 10% at the low injection pressure of 25 MPa but it does not have a significant effect on the discharge coefficient (less than 1%) at higher pressure differences of 85–175 MPa. Moreover, fuel density varying from 683 to 876 kg/m^3 is identified as the only property driving the mass flow rate, the theoretical evolution of which versus the square root of fuel density represents the discontinuous line.

The engine tests [23] showed that the higher flow pressure of viscous RO can damage microporous radial vee-shaped filtering cartridges. The flow capacity of the filter system can be enhanced by an arrangement of two or three identical filter units in parallel. A larger active surface area together with on-board heating of RO up to 60 °C would be the

solution to reduce viscosity and differential pressure across the filters and thus achieve the needed oil flow capacity. Additionally, variation in the viscosity of the liquid often changes its surface tension as well [24]. Apart from this problem, due to the chemical properties of rapeseed oil, the cetane improver is not as active as expected and only slightly helps to reduce an ignition delay [25].

A major purpose of the research in recent years was to improve the engine thermal efficiency and reduce emissions from the combustion of alternative and renewable fuels. However, the challenging issues in engine operating conditions inspired to retrospectively investigate the influence of the widely dissimilar physical properties of renewable fuels such as pure RO on the injection process and the spray macroscopic characteristics to attain more evidential facts about what qualitative and quantitative changes occur in the spray development after the start of injection. Comparative evaluation of new data attained with diesel fuel, pure RO and their blends may put more light on the changes in the spray macroscopic characteristics due to the higher density, viscosity, and surface tension of RO under identical injection pressure, back pressure, and the temperature conditions in the spray chamber with the non-operative environment.

The literature review showed (Table 1) that a greater part of studies continues to analyze diesel fuel spray characteristics [26–30], and biodiesel [6,12,14,19,31], but only a few of them were focused on the spray behavior of pure rapeseed oil [7], vegetable oils and animal fats [11,12]. The injection and spray macroscopic characteristics of RO are still not fully identified. The high density, viscosity and surface tension of RO may affect the macroscopic spray characteristics which must be compatible with the combustion chamber design and operating conditions to verify fuel efficiency and exhaust emissions.

Table 1. Summary of the most important referred literature.

Sr. No	Authors	Tested Fuels	Outcome
1.	Han D. et al. [6], Payri R. et al. [17], Salvador F.J. et al. [18], Boundy F. et al. [21], Dernotte J. et al. [22]	Biodiesels	Effect of fuel properties on injection characteristics
2.	Xie H. et al. [14], Bohl T. et al. [19], Ghurri A. et al. [20], Galle J. et al. [11]	Biodiesel	Effect of fuel properties on spray characteristics
3.	Galle J. et al. [11], Das M. et al. [12]	RO, PO, Castor oil, sunflower oil	Effect of fuel properties on spray and atomization characteristics
4.	Voijtišek-Lom M. et al. [7]	Crude rapeseed oil	Behaviour of DF and RO in tractor diesel engine with in-line injection pump
5.	Ettl et al. [8]	Crude rapeseed oil	Diesel engine performance and durability
6.	Zhang P. et al. [13]	Oxygenated fuels	Fuel spray and atomization characteristics

The purpose of the study was to investigate the changes in the fuel mass (volume) flow rate and the spray macroscopic characteristics such as the spray tip penetration length, spray cone angle, and spray area for diesel fuel (DF), straight rapeseed oil (RO), and their blends RO25, RO50 and RO75 injected by different injection pressures into an optically accessible chamber occupied with pressurized nitrogen gas (N_2) to ensure a fixed back pressure at an ambient temperature searching for the relationships between the spray macroscopic parameters and the widely differing fuel physical properties (density, viscosity, surface tension) under non-evaporating conditions. The injection characteristics were measured using an injection rate indicator based on the Bosch method and spray characteristics—using a spray visualization system.

2. Materials and Methods

This section presents a description of the experimental setup and procedures performed in the experiments. The following methodology, equipment and test procedures have been used to achieve the purpose of the research.

The measurements of the injection and spray characteristics and data analysis were performed for normal diesel as the reference fuel (DF), straight rapeseed oil (RO) and (DF75% + RO25%) RO25, (DF50% + RO50%) RO50 and (DF25% + RO75%) RO75 blends (by volume). The normal automotive diesel fuel (class 1) used in the study was produced by the refinery "Orlen Lietuva" and met the quality parameters specified in standard EN-590:2009 + A1. The composition of the diesel fuel was C/H = 0.8608/0.1299, with a residue 0.0093 containing traces of sulfur and water detected at the refinery's laboratory. The rapeseed oil used in the experiments was sourced from the RME production factory 'Rapsoila' in Mažeikiai and met the quality requirements specified in standard DIN 51605:2020-11 for use in agricultural machinery [2]. The elementary composition of RO was as follows: 77.2% carbons, 11.9% hydrogen and 10.9% oxygen. RO includes complicated long-side chains of fatty acids. Its density is 10% and surface tension 60.5% higher, respectively, than those of diesel fuel. The viscosity of RO at 40 °C is even 17.5 times higher than that of diesel fuel. The main properties of RO, diesel fuel and their blends are listed in Table 2.

Table 2. The main properties of the tested fuels.

Fuel Properties	Diesel	RO25	RO50	RO75	RO
Density at 15 °C, kg/m^3	831.1	851.8	872.5	893.3	914.0
Kinematic viscosity at 40 °C, mm^2/s	2.72	5.58	10.62	22.22	47.58
Surface tension, mN/m	36.0	41.2	46.7	52.4	57.8

The miscibility of RO with the diesel fuel is good to produce a stable mixture [32]; therefore, no co-solvents were used to avoid any contributing effect on the macroscopic spray characteristics. The fuel mixtures were prepared by mechanically mixing diesel fuel and rapeseed oil in the appropriate proportions.

Figure 1 shows a schematic diagram and photo of the injection rate measuring system consisting of the fuel injection system and the injection rate measuring system. The fuel injection system consisted an electrically driven high-pressure pump, a rail, an injector, and an injection pressure control unit. A standard Bosch solenoid injector (0 445 120 141) with 0.24 mm 6 hole nozzle (DLLA140P1790) was used for this study. The NI PXIe 1062Q system with NI-9751 C series module was used as a driver to control the injector's energizing duration. The injector was controlled by a peak current of 26.0 A and a hold current of 14.0 A.

The fuel injection rates were measured and analyzed using an injection rate measuring system based on the Bosch method [33]. The measurement concept is based on measuring a change in pressure by the fuel injection into a long measuring tube filled with fuel. This pressure change is proportional to the fuel injection rate:

$$\dot{m} = Const \cdot p(t), \quad (1)$$

$$Const = \frac{A_{tube}}{a} = \frac{m}{\int p(t)dt} \quad (2)$$

where

$\dot{m}$—mass injection rate;
A_{tube}—cross-sectional area of the measuring tube;
a—sound velocity in the fuel;
m—injected fuel mass;
$p(t)$—pressure variation.

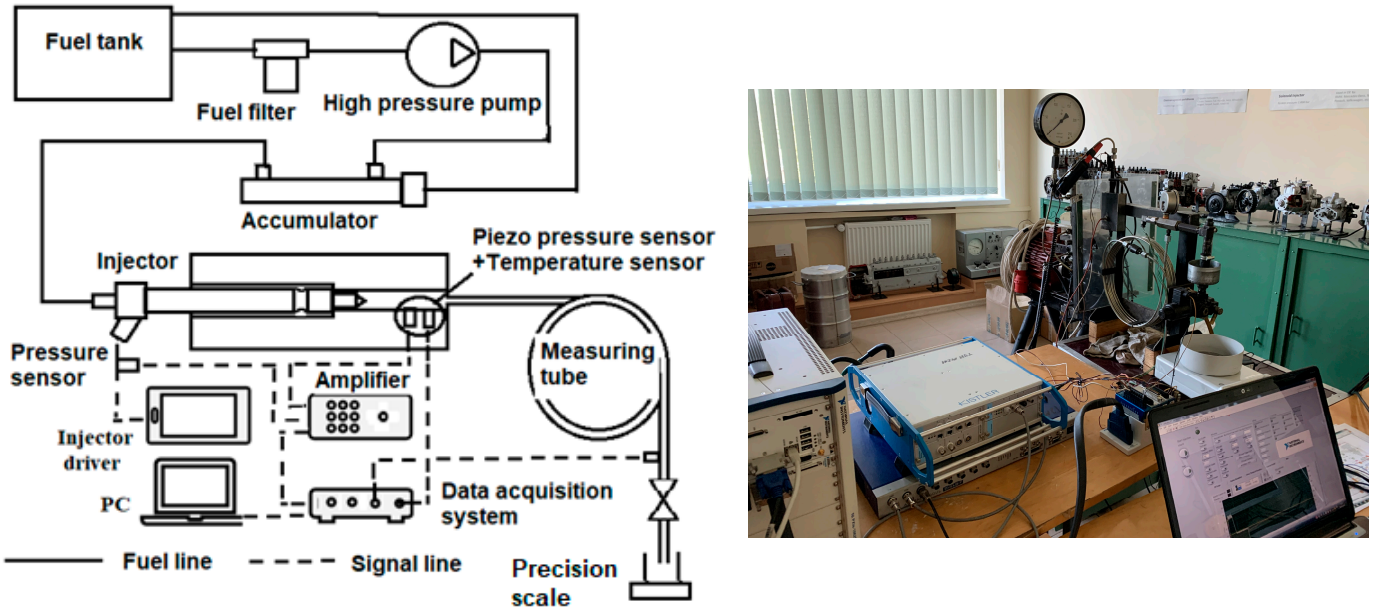


Figure 1. Schematic diagram and photo of the injection rate measuring systems.

The pressure variation in the tube was measured using a Kistler type 6052C piezoelectric pressure sensor (Kistler) (measuring range 0–150 bar, <±0.5%) coupled to a Kistler charge amplifier module 5064. The fuel pressure at the injector inlet was measured using a high-pressure Kistler Inc. piezoresistive sensor 4067A2000 (measuring range 0–2000 bar, <±0.5%) the signal of which was being amplified by an amplifier module 4665. Both amplifier modules were mounted on the signals conditioning platform compact 2854A. The signals of injector energizing, injection rate, fuel pressure and back pressure were recorded using an AVL IndiModul 622 data acquisition device. The mass of injected fuel was obtained from the mean value of 1000 continuous injections measured by a precision scale Kern 572-31 (weighing capacity 300 g, ±0.005 g).

The fuel temperature inside the measurement tube was measured using a Pt100 sensor (measure range −30–+180 °C, uncertainty ±0.8 °C) and controlled within a range of 308 ± 5 K. The injection pressure varied from 24 MPa to 80 MPa and the energizing duration was adjusted to ensure that the same amount of fuel (70 mm^3) was injected, regardless of the type of fuel (Table 3). The pressure in the measurement tube (back pressure) was adjusted to 4.0 MPa. The results of 100 consecutive injection cycles were recorded and averaged for analysis. The average standard deviation of the injection rate is presented in Table 4.

Table 3. Test matrix for injection rate and spray macroscopic characteristics measurement.

	Injector Energizing Duration, ms				
Injection Pressure	**DF**	**RO25**	**RO50**	**RO75**	**RO**
24.0 MPa	2.60	2.65	2.80	3.25	3.30
40.0 MPa	1.85	1.50	2.00	2.10	2.20
60.0 MPa	1.35	1.40	1.45	1.55	1.70
80.0 MPa	1.10	1.20	1.25	1.30	1.40

Measurements of macroscopic spray characteristics were performed under non-evaporating conditions in a specially designed spray chamber (Figure 2). A medium-pressure stainless steel constant-volume chamber was constructed and produced for this purpose. The chamber had a diameter of 110 mm and was equipped with an optical accessible window.

Table 4. The averaged standard deviation of the injection rate.

	Standard Deviation, mg				
Injection Pressure	**DF**	**RO25**	**RO50**	**RO75**	**RO**
24.0 MPa	±0.463	±0.730	±0.879	±0.906	±0.756
40.0 MPa	±0.450	±0.712	±0.807	±0.901	±0.716
60.0 MPa	±0.641	±0.779	±0.889	±0.868	±0.771
80.0 MPa	±0.864	±0.836	±0.905	±0.904	±0.749

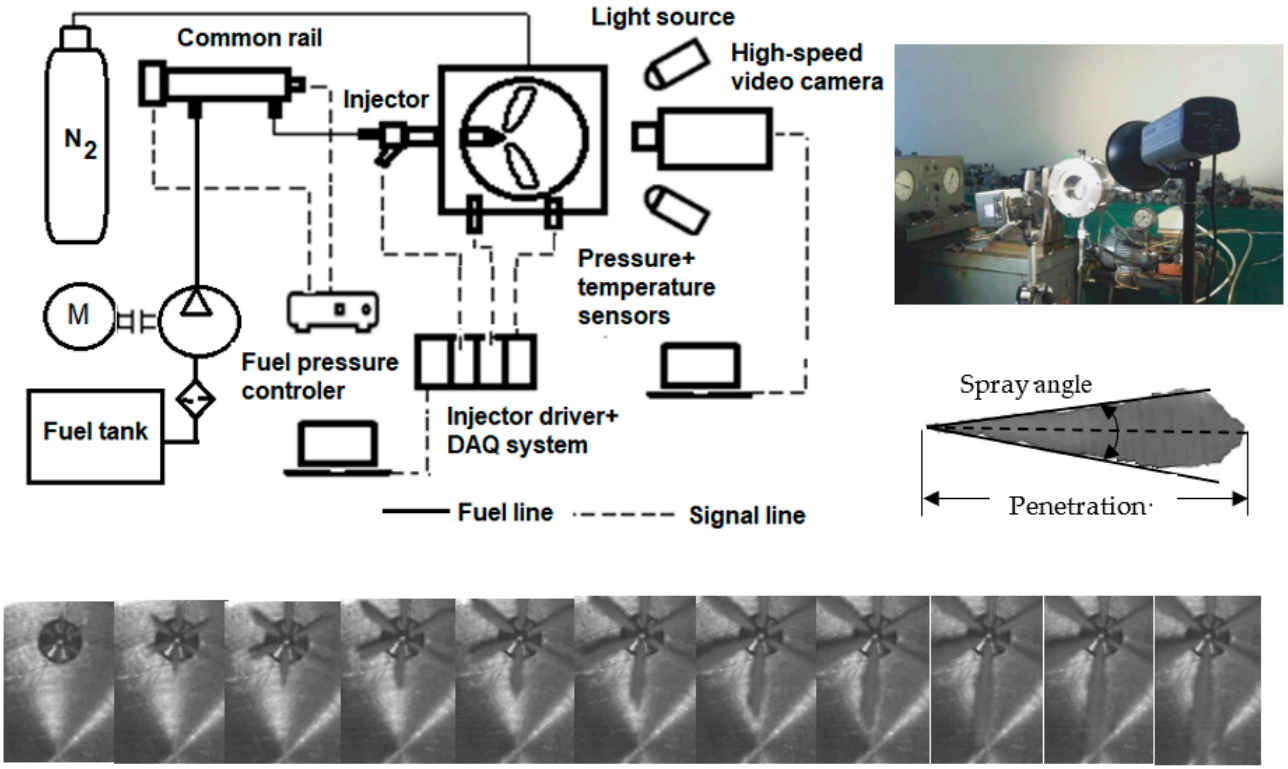


Figure 2. Fuel spray capturing setup and example of captured images sequence.

The spray chamber was filled with inert gas nitrogen (N_2) from a high-pressure vessel to a constant back pressure of 4.0 MPa, which was controlled with a pressure regulator valve. The temperature inside the spray chamber also was kept at a constant level of 20 °C to ensure non-evaporating test conditions. After each measurement, the nitrogen was re-placed to reduce the volume of fuel vapors and thus improve visibility through the chamber window.

The fuel injection system used in this experiment was similar to that used in the injection rate measurement system. A National Instrument CompactRIO system with a real-time controller and necessary modules has been used to control the system and measure gas parameters. For this purpose, special software in the LabView environment has been designed and used.

High-speed video camera PHOTRON FASTCAM-1024PCI was used to capture images of fuel sprays at capturing speed of 18,000 frames per second. The following measurements were analyzed from the images: spray tip penetration, spray width, and spray cone angle. The surface area was calculated using these resulting measurements. The analysis of images and measurements has been produced by the software NI "Vision Assistant 2010". For each mode, the images of 10 injections were analyzed. Spray tip penetration was defined as the distance from the nozzle exit to the furthest point of the spray. The average standard deviation of the spray tip penetration is presented in Table 5. The spray cone angle was

defined as the angle formed by two straight lines drawn from the discharge orifice and touching the first 60% of the spray contour. The spray area was defined as the vertically projected area of the spray to the plane.

Table 5. The overaged standard deviation of the spray tip penetration.

	Standard Deviation, mm				
Injection Pressure	**DF**	**RO25**	**RO50**	**RO75**	**RO**
24.0 MPa	±1.145	±0.960	±0.665	±0.698	±0.716
40.0 MPa	±1.196	±0.864	±1.121	±0.743	±0.785
60.0 MPa	±0.826	±0.718	±0.839	±1.094	±0.873
80.0 MPa	±0.735	±1.124	±0.824	±0.677	±0.670

The test conditions were like that for injection rate measuring (Table 3).

3. Results and Discussion

In this section, a discussion of the experimental results of a study of injection and fuel spray characteristics obtained with normal diesel fuel (DF), pure rapeseed oil (RO) and their RO25, RO50 and RO75 blends are presented.

The structural differences in the RO composition, its high density, viscosity, and surface tension may affect injection and spray characteristics causing lower injection rate, poor atomization and uneven distribution of injected oil in a combustion chamber. The miscibility of straight vegetable oils with diesel fuel is good and all vegetable oils suggested normal DI diesel engine operation without problems during the short-term experiments [34]. Besides, the use of RO demonstrated better than sunflower and cottonseed oils behavior as an alternative fuel to DF in the agricultural tractor engine.

3.1. Injection Rate Characteristics

The fuel injection process in a diesel engine plays a crucial role in the in-cylinder combustible mixture formation, ignition, combustion, and formation of harmful emissions. Figure 3a,b present the volume (a) and mass (b) injection rates as a function of time after injector energizing for diesel fuel (DF), fuel blends RO25, RO50, RO75 and pure (100%) rapeseed oil (RO). The flow rates of the fuels are recorded for injection pressures of 24.0, 40.0, 60.0 and 80.0 MPa at a constant back pressure of 4.0 MPa and the respective energizing times selected within an interval of 3.30–1.10 ms to ensure the same fuel volume injected per cycle.

The peak volumetric injection rates of RO and its blends with DF were lower compared to diesel fuel. By injection of the same amount of fuel, the peak injection rates of RO were 22.0, 20.6, 11.3 and 9.1% lower with a group of fuel blends RO25, RO50 and RO75 positioned in decreasing flow rate order between DF and RO for the injection pressures of 24.0, 40.0, 60.0 and 80.0 MPa, correspondently (Figure 3a). The changes in flow rate, caused by the widely dissimilar properties of RO, impact the entire injection process. As the injection pressure increases, the maximum injection rate also increases, and the time to reach the maximum injection rate was advanced for all fuel tested. A similar effect on the injection rate of such fuel properties as density and viscosity was also found by other researchers who studied the characteristics of FAME injection [17,18,21].

As shown in Figure 3, the injection rate of diesel fuel exhibits the steepest rising slope at the beginning of injection, while RO shows a smoother injection rate shape, potentially due to their viscosities slowing down the needle lift process, as also observed by Dong Han et al. [6].

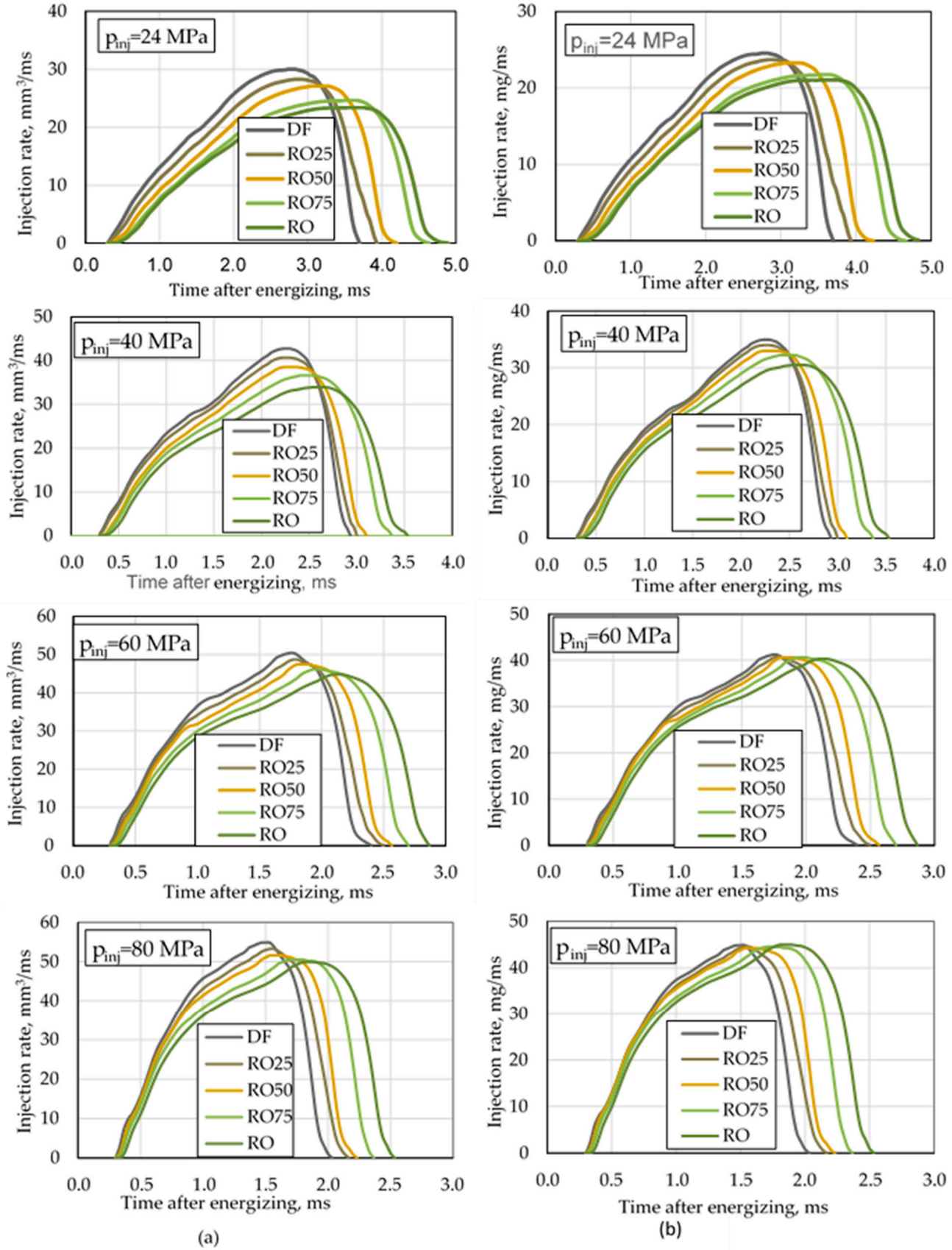


Figure 3. The fuel volumetric (**a**) and mass (**b**) flow rates as a function of time after injector energizing for injection pressures of 24.0, 40.0, 60.0, and 80.0 MPa.

All injection delay data fall within a range between 0.3 ms and 0.47 ms. The injection delay is defined as the time interval between the start of the energizing signal and the start of fuel injection from the nozzle. It can be seen in the graphs, the diesel fuel portions appear at first, followed in increasing order by fuel blends RO25, RO50, RO75 and RO (100%). A trivial decrease is observed with increased injection pressure, as higher fuel pressure provides a greater force to lift the needle. The actual injection durations for all tested fuels were approximately 30, 39, 48 and 54% longer than the energizing durations for the injection pressures of 24.0, 40.0, 60.0 and 80.0 MPa, correspondently. The injection lasts longer than the control pulse because, after the control valve closes, it takes some time for the fuel to fill the control chamber and generate enough force to press the nozzle needle to the seat. This delay is influenced by the fuel's density and viscosity as well as the injection pressure.

It is important to stress that the impact of cavitation on internal flow and fuel flow rate may be less damaging when using dense and viscous vegetable oil rather than diesel fuel. Lamoot et al. [35] reviewed literature from the past fifty years and highlighted the positive role of biofuels as a solution against the cavitation phenomenon. The higher viscosity of biofuels reduces the harmful effects of cavitation inside the injectors, allowing them to avoid significant damage and malfunctions. Consequently, the negative effect of cavitation on the flow within the injector, spray formation, and atomization of vegetable oil might be less critical, even for a cylindrical nozzle's hole.

Although the density of rapeseed oil is higher than that of diesel fuel (Table 2), the latter exhibits a higher mass injection rate than RO at lower injection pressures of 24.0 and 40.0 MPa, at the very least. The maximum mass flow rate of RO remains still 13.9% and 12.8% below that of diesel fuel at injection pressures of 24.0 and 40.0 MPa, respectively. The difference is clearly visible at the maximum flow rates when the needle is fully open, and the injection process is stable. This phenomenon makes a difference associated with the results obtained by Payri et al. [26] where the maximum mass flow rate of diesel fuel was approximately 6–7% higher than gasoline, which is the same value as the squire root of the densities. It should be noted that in that study the maximum injection pressures were 1200 and 1800 bar and, therefore, the effect of density, which was 13.6% higher than that of gasoline, on the mass flow rate could be relatively greater.

As could be expected (Figure 3b), the differences in maximum mass flow rates between diesel fuel, rapeseed oil and fuel blends become negligible at the higher injection pressures of 60.0 and 80.0 MPa due to the roughly 10% higher density of RO, which compensates for the lower volumetric flow rate. In fact, the higher the injection pressure, the greater the average values of volumetric and mass flow rates, as the needle-valve returns to the seat more quickly and the time available to inject the same fuel quantity becomes extremely limited (Figure 3a,b).

3.2. Spray Characteristics

Figure 4 shows the spray tip penetration of diesel fuel, rapeseed oil and the three DF-RO blends for different injection pressures of 24.0, 40.0, 60.0 and 80.0 MPa at a constant (4.0 MPa) back pressure in the spray chamber (not all points are plotted for better distinction of the curves). The time scale represents the time after the start of energizing, as such a technique allows for superimposing the start of injection (SOI) of all the fuels, regardless of whether the hydraulic delay of each fluid is dissimilar [26]. As the study intends to show the differences in spray tip penetration (STP) and cone angle caused by the vastly different physical properties of the fuels, the spray macroscopic characteristics for all the injection pressures start at the SOI point. As a result, the small hydraulic delay between the energizing impulse and the onset of spray tip penetration is not depicted on the graphs. Because all characteristics are time-adjusted and the first droplets of each fuel appear simultaneously, applying such a technique simplifies the data analysis.

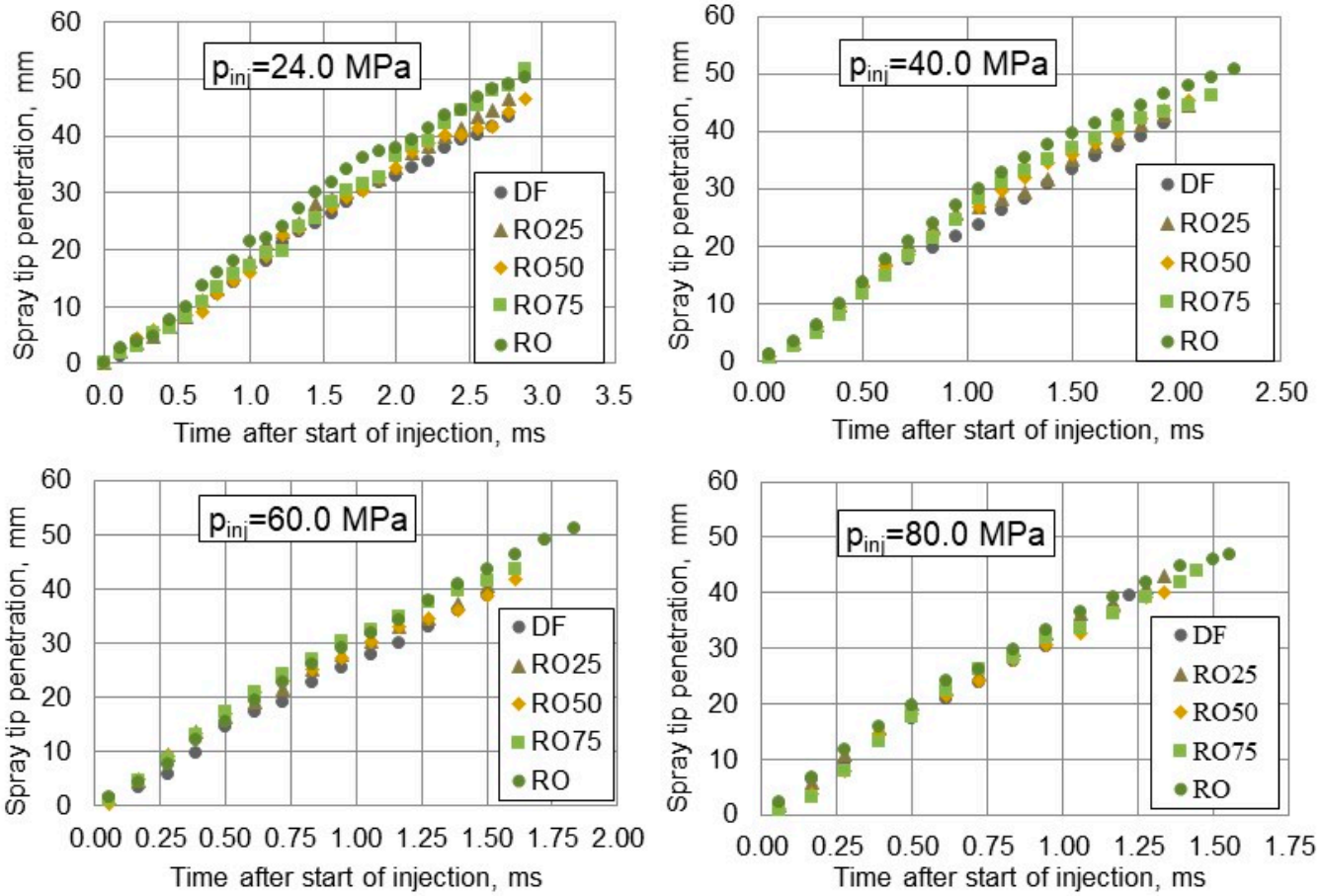


Figure 4. The spray tip penetration as a function of time after the start of injection.

Analysis of the data showed that at the beginning of injection, the spray tip penetration of all tested fuels is nearly identical. Galle et al. [11] tested the penetration of diesel and biodiesel and also revealed that during the early stages of spray formation, the penetration is quite similar for all fuels. One millisecond after the start of injection, the spray tip penetration was 26.9, 25.5, 14.0 and 7.4% longer for pure RO than for diesel fuel at the respective injection pressures of 24.0, 40.0, 60.0 and 80.0 MPa. The RO spray develops faster than that of the diesel because RO is dense and viscous, resulting in a larger droplet diameter and higher momentum to penetrate the compressed ambient gas. The spray tip penetrations of fuel blends RO25, RO50 and RO75 were in decreasing order between DF and RO (Figure 4). Whereas, as both the injection rate and the spray development increased at an injection pressure of 80.0 MPa, the changes in the spray tip penetrations diminished, making it difficult to detect significant differences in the spay development of various fuel blends.

Figure 5 illustrated the spray evolution process of all tested fuels at two injection pressures. It can be seen that the difference in spray tip penetrations of the tested fuel jets is more noticeable at lower pressure. Additionally, it can be observed that the spray cone angle decreases with increasing rapeseed oil content in the fuel.

The test results indicated that rapeseed oil, having the highest density among the tested fuels, achieved the longest spray tip penetration. However, as a trade-off, it produced the smallest spray cone angle, which may result in a more unevenly distributed air-oil mixture in the chamber (Figure 6).

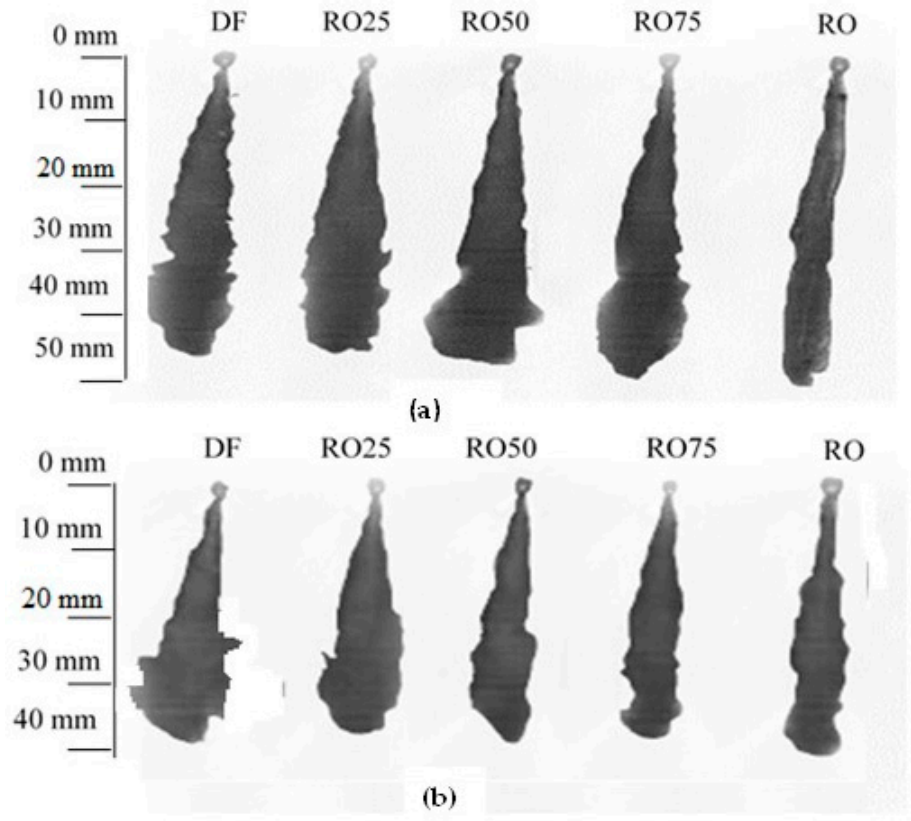


Figure 5. Spray evolution of diesel fuel, rapeseed oil and its blend: (**a**) at 40.0 MPa injection pressure and 2 ms after the start of injection; (**b**) at 80 MPa injection pressure and 1 ms after the start of injection.

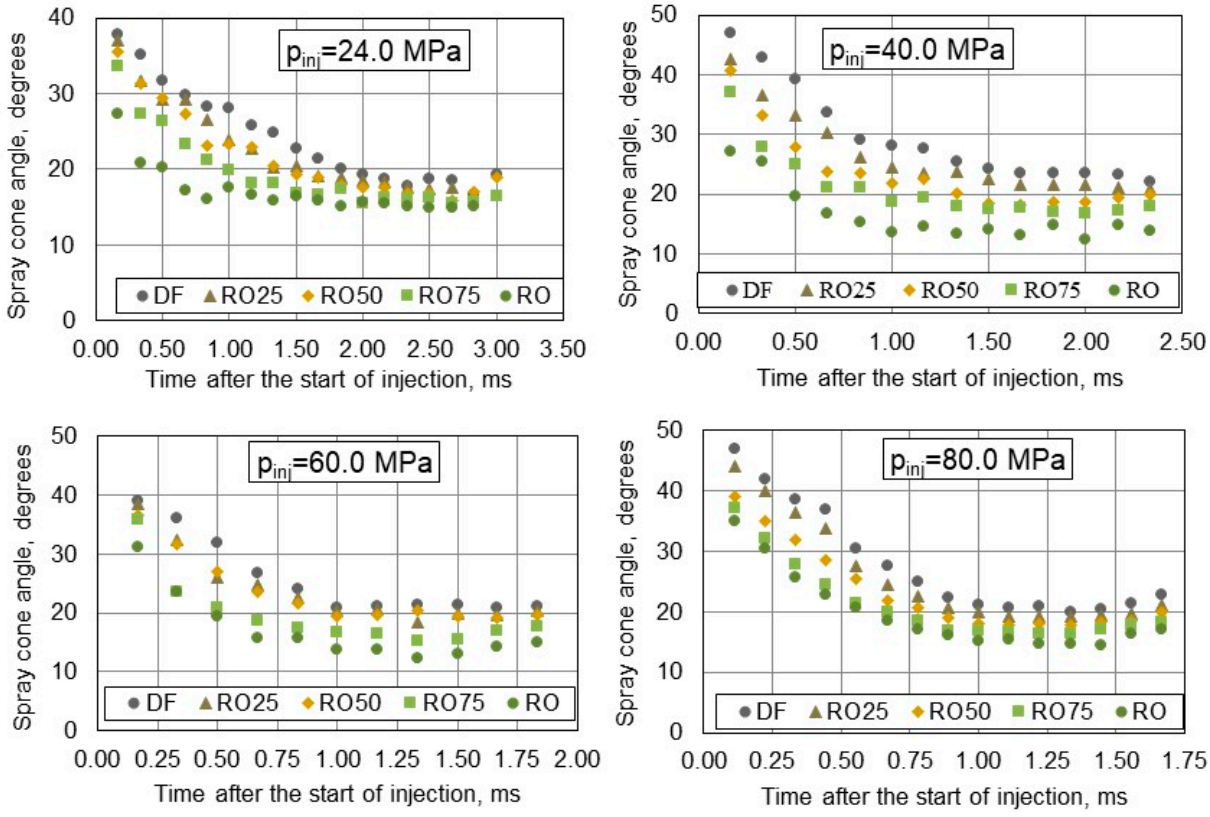


Figure 6. Development of the spray cone angle as a function of time after the start of injection.

The spray cone angle of rapeseed oil at 1 ms after the start of injection was 17.6°, which is 1.6 times smaller than the 28.2° diesel fuel produces for the injection pressure of 24.0 MPa (Figure 6). Spray angles developed within 0.5 to 1 ms after the SOI for fuel blends RO25, RO50 and RO75 were also in increasing order 6.4%, 13.5% and 20.2% lower than the diesel fuel develops under identical injection conditions. The smaller spray angle of RO with larger (viscosity, surface tension) and heavier (density) droplets experienced lower deceleration and produced higher momentum to overcome back pressure (Figure 4). Therefore, penetration length increased while the spray cone angle decreased with increasing RO content due to the higher density and viscosity of fuel blends causing poor atomization. Bohl et al. [18] study on spray characteristics of hydrotreated vegetable oil and vegetable oil methyl esters shows a similar effect of fuel density on spray cone angle. After reaching the maximum during the early injection stage, the spray cone angle of all tested fuels slowly decreases and then remains stable.

Even though the differences in the spray macroscopic characteristics diminish with the injection pressure increased to 40.0, 60.0 and 80.0 MPa, the spray cone angles of diesel fuel were high enough while the respective angles of viscous RO were 50.1%, 37.3% and 31.7% lower in a time interval from 0.5 to 1 ms after the start of injection, with spray cone angles of fuel blends distributed between them. A study on the effect of physical properties of residual fuel oil (RFO) on the spray parameters also showed that the relationship between the viscosity and spray cone angle is inversely proportional at higher viscosity values and increases monotonously within the range of diesel fuel at lower viscosity values [15]. The spray angles become smaller for a time longer than 1 ms and the differences in the cone angles between the fuels of various origins diminish to some extent, along with the disintegration of the spray occurring earlier after the SOI at the higher injection pressures. In the steady-state spray angle, the differences diminish and when the injection pressure is sufficiently high, the spray angle no longer depends on the injection pressure [11].

Figure 7 presents the projected spray area as a function of the spray length of diesel fuel (DF) and rapeseed oil (RO) for all injection pressures of 24.0, 40.0, 60.0 and 80.0 MPa at a back pressure of 4.0 MPa in the spray chamber. The larger the spray area of the fuel, the better the air-fuel mixing quality would be expected with a more widely distributed plume of fuel droplets and thus fuel-efficient and clean combustion. Although the spray area generally demonstrates a linear trend as a function of time for all the fuels [19], to emphasize the difference, the spray area per injected mass is consistently lower for rapeseed oil than for lighter diesel fuel produces at the same spray tip penetration length. Consequently, the test results confirm that rapeseed oil has poorer air-fuel mixing quality than conventional diesel under the same injection conditions.

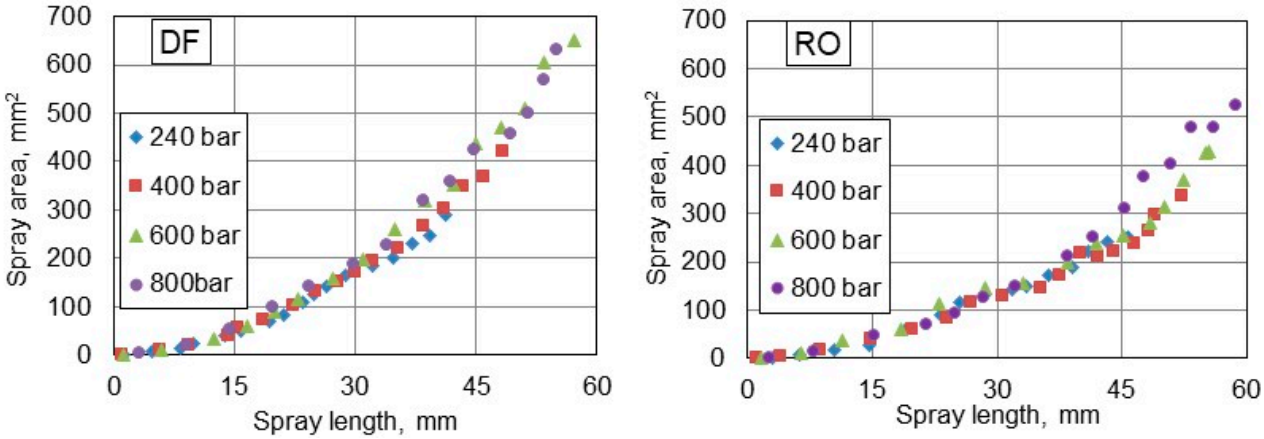


Figure 7. Spray area as a function of the spray length.

The spray area difference for the same spray length between diesel fuel and rapeseed oil is greater at higher injection pressure at constant back pressure (4.0 MPa) and the temperature (293 K) in the chamber. The spray area for diesel fuel is less dependent on the

injection pressure difference and remains within a narrow variation range of 460–500 mm^2 for the same (50 mm) penetration length, while the spray plume area for RO is consistently (31.8–20.0%) lower and changes within a wider range of 300–400 mm^2 under identical test conditions. The results obtained confirm that the spray cone angle is a crucial factor since, for diesel fuel, it is consistently higher, and the spray area is also larger than that of RO for the same spray tip penetration developed under non-evaporating conditions. Therefore, it can be assumed that rapeseed oil and its blends with diesel tend to produce poor initial air-fuel mixture distribution, resulting in a lower fuel portion premixed for ignition and rapid premixed combustion compared to conventional diesel fuel.

4. Conclusions

In this study, the injection processes and spray behavior of diesel fuel, rapeseed oil and their fuel blends have been qualitatively and quantitatively analyzed to identify the differences in the injection rate and the spray parameters. The volumetric and mass injection rates, the spray penetration, the spray cone angle, and the spray area under non-evaporation conditions in a nitrogen-filled camber were analyzed. The following conclusions can be drawn from this investigation:

1. Compared to diesel fuel, the peak volumetric injection rate of rapeseed oil was 22.0, 20.6, 11.3 and 9.1% lower by injection of the same amount of fuel at the injection pressure of 24.0, 40.0, 60.0 and 80.0 MPa, correspondently. Moreover, rapeseed oil and its blends with diesel fuel show a slower rise in the volumetric injection rate after the start of injection caused by its higher density and viscosity. Despite the higher density of rapeseed oil and its blend with diesel fuel, at low pressure, their mass flow rates remain lower than that of diesel fuel. The differences in maximum mass flow rates between diesel fuel, rape-seed oil and fuel blends become negligible at the higher injection pressures of 60.0 and 80.0 MPa due to about 10% higher density of RO that compensates for the lower volumetric flow rate.
2. The spray development of RO demonstrates 26.9, 25.5, 14.0 and 7.4% longer tip penetration than diesel fuel at the injection pressures of 24.0, 40.0, 60.0 and 80.0 MPa after the same time after the start of injection (1 ms). The spray tip penetrations of the fuel blends RO25, RO50 and RO75 were arranged between the values of DF and RO. As the injection pressure increases the differences in the spray tip penetrations diminish.
3. The spray cone angle of RO was 61.4%, 50.1%, 37.3% and 31.7% smaller than diesel fuel develops for the injection pressures of 24.0, 40.0, 60.0 and 80.0 MPa in the spray chamber. The fuel blends suggest smaller cone angles than diesel. The spray cone angles increase to maximum just after the start of injection and then decrease and stabilize around lower values.
4. The spray area of RO is always 32.0–20.0% lower than that of diesel fuel and varies within a wide range of 300 to 400 mm^2 while the spray area of diesel fuel less depends on the variation of injection pressure from 24.0 to 80.0 MPa and changes within a narrow range 460–500 mm^2 for the same spray tip penetration of 50 mm. A smaller spray area would be expected to provide a poor distribution of RO droplets.

The noted changes in the spray macroscopic characteristics of pure rapeseed oil and its blends with diesel fuel can be reasonably applied to sunflower, cottonseed and other vegetable oils since their physical properties do not differ much from those.

Funding: This research received no external funding.

Institutional Review Board Statement: Not applicable.

Informed Consent Statement: Not applicable.

Data Availability Statement: Not applicable.

Conflicts of Interest: The author declares no conflict of interest.

Abbreviations

The following abbreviations and acronyms are used in this manuscript.

CO_2	Carbon dioxide
GHG	Greenhouse Gases
FAME	Fatty Acid Methyl Esters
LCA	Life Cycle Assessment
DF	Diesel Fuel
RO	Rapeseed Oil
RO25	75% Diesel Fuel + 25% Rapeseed Oil
RO50	50% Diesel Fuel + 50% Rapeseed Oil
RO75	75% Diesel Fuel + 25% Rapeseed Oil
SOI	Start of Injection
STP	Spray Tip Penetration

References

1. Holden, N.M.; Wolfe, M.L.; Ogejo, J.A.; Cummins, E.J. *Introduction to Biosystems Engineering*; American Society of Agricultural and Biological Engineers (ASABE) and Virginia Technical Publishing: St. Joseph, MI, USA, 2021; Volume 3, pp. 154–196. [CrossRef]
2. *DIN 51605:2020-11*; Kraftstoffe für Pflanzenöltaugliche Motoren—Rapsölkraftstoff—Anforderungen und Prüfverfahren/Fuels for Vegetable Oil Compatible Combustion Engines—Fuel from Rapeseed Oil—Requirements and Test Methods. DIN: Berlin, Germany, 2020; p. 18. [CrossRef]
3. Fridrihsone, A.; Romagnoli, F.; Cabulis, U. Environmental life cycle assessment of rapeseed and rapeseed oil produced in Northern Europe: A Latvian case study. *J. Sustain.* **2020**, *12*, 5699. [CrossRef]
4. Mizik, T.; Gyarmati, G. Economic and sustainability of biodiesel production—A systematic literature review. *J. Clean Technol.* **2021**, *3*, 19–36. [CrossRef]
5. Lefebvre, A.H.; McDonell, V.G. *Atomization and Sprays*, 2nd ed.; eBook; CRC Press: Boca Raton, FL, USA, 2017; p. 300. [CrossRef]
6. Han, D.; Duan, Y.; Wang, C.; Lin, H.; Huang, Z. Experimental study on injection characteristics of fatty acid esters on a diesel engine common rail system. *Fuel* **2014**, *123*, 19–25. [CrossRef]
7. Vojtišek-Lom, M.; Pechout, M.; Barbolla, A. Experimental investigation of the behaviour of non-esterified rapeseed oil in a diesel engine mechanical fuel injection system. *Fuel* **2012**, *97*, 157–165. [CrossRef]
8. Ettl, J.; Bernhardt, H.; Huber, G.; Thuneke, K.; Remmele, E.; Emberger, P. Evaluation of pure rapeseed oil as a renewable fuel for agricultural machinery based on emission characteristics and long-term operation behaviour of a fleet of 18 tractors. *SN Appl. Sci.* **2020**, *2*, 1711. [CrossRef]
9. Aguado-Deblas, L.; Hidalgo-Carrillo, J.; Bautista, F.M.; Luna, C.; Calero, J.; Posadillo, A.; Romero, A.A.; Luna, D.; Estévez, R. Biofuels from Diethyl Carbonate and Vegetable Oils for Use in Triple Blends with Diesel Fuel: Effect on Performance and Smoke Emissions of a Diesel Engine. *Energies* **2020**, *13*, 6584. [CrossRef]
10. Hanna, R.; Zoughaib, A. Atomization of high viscosity liquids through hydraulic atomizers designed for water atomization. *Exp. Therm. Fluid Sci.* **2017**, *85*, 140–153. [CrossRef]
11. Galle, J.; Defruyt, S.; Van de Maele, C.; Rodriguez, R.P.; Denon, Q.; Verliefde, A.; Verhelst, S. Experimental investigation concerning the influence of fuel type and properties on the injection and atomization of liquid biofuels in an optical combustion chamber. *Biomass Bioenergy* **2013**, *57*, 215–228. [CrossRef]
12. Das, M.; Sarkar, M.; Datta, A.; Santra, A.K. Study on viscosity and surface tension properties of biodiesel-diesel blends and their effects on spray parameters for CI engines. *Fuel* **2018**, *220*, 769–779. [CrossRef]
13. Zhang, P.; Su, X.; Yi, C.; Chen, H.; Xu, H.; Geng, L. Spray, atomization and combustion characteristics of oxygenated fuels in a constant volume bomb: A review. *J. Traffic Transp. Eng.* **2020**, *7*, 282–297. [CrossRef]
14. Xie, H.; Song, L.; Xie, Y.; Pi, D.; Shao, C.; Lin, Q. An Experimental Study on the Macroscopic Spray Characteristics of Biodiesel and Diesel in a Constant Volume Chamber. *Energies* **2015**, *8*, 5952–5972. [CrossRef]
15. Ogunedo, M.B.; Nduaguba, K.C. Effect of Fuel Physical Properties on Spray Parameters of Residual Fuel Oil (RFO). *IJRR Int. J. Res. Rev.* **2019**, *6*, 448–456.
16. Wang, Z.; Ding, H.; Wyszynski, M.L.; Tian, J.; Xu, H. Experimental study on diesel fuel injection characteristics under cold start conditions with single and split injection strategies. *Fuel Process. Technol.* **2015**, *133*, 213–222. [CrossRef]
17. Payri, R.; Salvador, F.J.; Martí-Aldaraví, P.; Martínez-López, J. Using one-dimensional modeling to analyse the influence of the use of biodiesels on the dynamic behavior of solenoid-operated injectors in common rail systems: Detailed injection system model. *Energy Convers. Manag.* **2012**, *54*, 90–99. [CrossRef]
18. Salvador, F.J.; Gimeno, J.; De la Morena, J.; Carreres, M. Using one-dimensional modeling to analyze the influence of the use of biodiesels on the dynamic behavior of solenoid-operated injectors in common rail systems: Results of the simulations and discussion. *Energy Convers. Manag.* **2012**, *54*, 122–132. [CrossRef]
19. Bohl, T.; Tian, G.; Smallbone, A.; Roskilly, A.P. Macroscopic spray characteristics of next-generation bio-derived diesel fuels in comparison to mineral diesel. *Appl. Energy* **2017**, *186*, 562–573. [CrossRef]

20. Ghurri, A.; Kim, J.-D.; Kim, H.G.; Jung, J.-Y.; Song, K.-K. The effect of injection pressure and fuel viscosity on the spray characteristics of biodiesel blends injected into an atmospheric chamber. *J. Mech. Sci. Technol.* **2012**, *26*, 2941–2947. [CrossRef]
21. Boudy, F.; Seers, P. Impact of physical properties of biodiesel on the injection process in a common-rail direct injection system. *Energy Convers. Manag.* **2009**, *50*, 2905–2912. [CrossRef]
22. Dernotte, J.; Hespel, C.; Foucher, F.; Houillé, S.; Mounaïm-Rousselle, C. Influence of physical fuel properties on the injection rate in a Diesel injector. *Fuel* **2012**, *96*, 153–160. [CrossRef]
23. Labeckas, G.; Slavinskas, S. Performance of direct-injection off-road diesel engine on rapeseed oil. *Renew. Energy* **2006**, *11*, 849–863. [CrossRef]
24. Shlegel, N.E.; Tkachenko, P.P.; Strizhak, P.A. Influence of viscosity, surface, and interfacial tensions on the liquid droplet collisions. *Chem. Eng. Sci.* **2020**, *220*, 115639. [CrossRef]
25. Labeckas, G.; Slavinskas, S. Comparative evaluation of the combustion process and emissions of a diesel engine operating on the cetane improver 2-Ethylhexyl nitrate doped rapeseed oil and aviation JP-8 fuel. *Energy Convers. Manag. X* **2021**, *11*, 100106. [CrossRef]
26. Payri, R.; Garcia, A.; Domenech, V.; Durrett, R.; Plazas, A.H. An experimental study of gasoline effects on injection rate, momentum flux and spray characteristics using a common rail diesel injection system. *Fuel* **2012**, *97*, 390–399. [CrossRef]
27. Payri, F.; Bermu'dez, V.; Payri, R.; Salvador, J. The influence of cavitation on the internal flow and the spray characteristics in diesel injection nozzles. *Fuel* **2004**, *83*, 419–431. [CrossRef]
28. Freitas, S.V.D.; Santos, Â.; Moita, M.-L.C.J.; Follegatti-Romero, L.A.; Dias, T.P.V.B.; Meirelles, A.J.A.; Daridon, J.-L.; Lima, Á.S.; Coutinho, J.A.P. Measurement and prediction of speeds of sound of fatty acid ethyl esters and ethylic biodiesels. *Fuel* **2013**, *108*, 840–845. [CrossRef]
29. Wang, Z. Experimental Study on Diesel Spray with Single and Multiple Injection under Room Temperature and Low Temperature. Ph.D. Thesis, University of Birmingham, Birmingham, UK, 2015; p. 253.
30. Postrioti, L.; Buitoni, G.; Pesce, F.C.; Ciaravino, C. Zeuch method-based injection rate analysis of a common-rail system operated with advanced injection strategies. *Fuel* **2014**, *128*, 188–198. [CrossRef]
31. Ejim, C.E.; Fleck, B.A.; Amirfazli, A. Analytical study for atomization of biodiesels and their blends in a typical injector: Surface tension and viscosity effects. *Fuel* **2007**, *86*, 1534–1544. [CrossRef]
32. Labeckas, G.; Slavinskas, S. Performance and exhaust emissions of direct-injection diesel engine operating on rapeseed oil and its blends with diesel fuel. In *Transport: Journal of Vilnius Gediminas Technical University and Lithuanian Academy of Sciences*; Technika: Vilnius, Lithuania, 2005; Volume 20, pp. 186–194.
33. Bosch, W. The fuel rate indicator: A new instrument for display of the characteristic of individual injection. *SAE Pap.* **1966**, 660749. [CrossRef]
34. Balafoutis, A.; Fountas, S.; Natsis, A.; Papadakis, G. Performance and emissions of sunflower, rapeseed, and cottonseed oils as fuels in an agricultural tractor engine. *Res. Artic. Int. Sch. Res. Netw. ISRN Renew. Energy* **2011**, *2011*, 12. [CrossRef]
35. Lamoot, L.; Manescau, B.; Chetehouna, K.; Gascoin, N. Review on the Effect of the Phenomenon of Cavitation in Combustion Efficiency, and the Role of Biofuels as a Solution against Cavitation. *Energies* **2021**, *14*, 7265. [CrossRef]

Disclaimer/Publisher's Note: The statements, opinions and data contained in all publications are solely those of the individual author(s) and contributor(s) and not of MDPI and/or the editor(s). MDPI and/or the editor(s) disclaim responsibility for any injury to people or property resulting from any ideas, methods, instructions or products referred to in the content.